

Study of the effects of growth rate, miscut direction and postgrowth argon annealing on the surface morphology of homoepitaxially grown 4H silicon carbide films

M. Camarda^{a,b}, A. Canino^{a,b}, P. Fiorenza^a, A. Severino^{a,b}, R. Anzalone^a,
S. Privitera^a, A. La Magna^a, F. La Via^a
C. Vecchio^b, M. Mauceri^b, G. Litrico^b, A. Pecora^b, D. Crippa^c

massimo.camarda@imm.cnr.it

^a Consiglio Nazionale delle Ricerche, Istituto di Microelettronica e
Microsistemi CNR-IMM, Z.I. VIII Strada 5 I 95121 Catania, Italy

^b Epitaxial Technology Center, XVI Strada, Pantano d'Arci, 95121 Catania, Italy

^c LPE spa, Via falzarego 8. 20021 Baranzate, Italy

Keywords: surface morphology, surface instabilities, step bunching

Abstract. we study the surface morphology of homoepitaxially grown 4H silicon carbide in terms of growth rate, miscut direction of the substrate and post growth argon thermal annealings. All the results indicate that the final surface morphology is the result of a competition between energetic reorganization and kinetic randomness. Because in all observed conditions energetic reorganization favors surface undulations (“step bunching”), out-of-equilibrium conditions are one of the keys to favor the reduction of the surface roughness to values below ~0.5 nm. We theoretically support these results using kinetics superlattice Monte Carlo simulations (KslMC).

Introduction

4H Silicon carbide films are usually grown on misoriented substrates, i.e. substrate with surfaces few degree off from the (0001) plane, to facilitate step-controlled epitaxial growth. However, due to surface steps, self ordering is commonly observed after thermal treatments, epitaxial growths or etching under suitable conditions. Various interesting phenomena related to step-and-terrace structures such as faceting[1], step bunching[2,3 ,4 ,5] and step meandering[6] are known to occur during epitaxial growths on misoriented substrates [7,8 ,9 ,10 ,11]. All these surface instabilities are of great interest from a viewpoint of not only crystal growth but also electronic engineering, because device performance is affected by “micro-roughness” at a junction interface or on the surface. This phenomenon is particularly critical in high-power devices where the junction interface can cause electric field crowding[12], negatively impacts the channel mobility[13] or the oxide breakdown characteristics in metal-oxide-semiconductor field effect transistors MOSFETs[14].

This nano-ordering is the result of a competition between two opposing tendencies: energetic (step-step attractive strain interaction[15,16], step reactivity[17,18 ,19]) which favours the re-organization in terms of nano-undulations and the generation of step meandering (zig-zag features of the steps, see Fig.3), and kinetic which, by increasing the overall randomness of the deposition, hinders it (see Fig.1). To explore the role of the surface kinetics on the final surface morphology we have studied two film grown under the same deposition conditions (on 4H-SiC 4° degree off <11-20> misoriented substrates at 1650° C/Si=1.1) but changing the growth rate, from 4 μm/h (*lowGr* sample) to 27 μm/h (*highGr* sample). Furthermore, to highlight the role of the crystallographic reconstruction on the step structure, we analyzed the surfaces of two films grown on <11-20> and <1-100> misoriented 4H-SiC substrates after high temperature (T=1650°C) low-pressure (20 mbar) argon annealing. Finally we compared the experimental results on the growth rate with 3D kinetic Monte Carlo simulations on super-lattices [20,21].

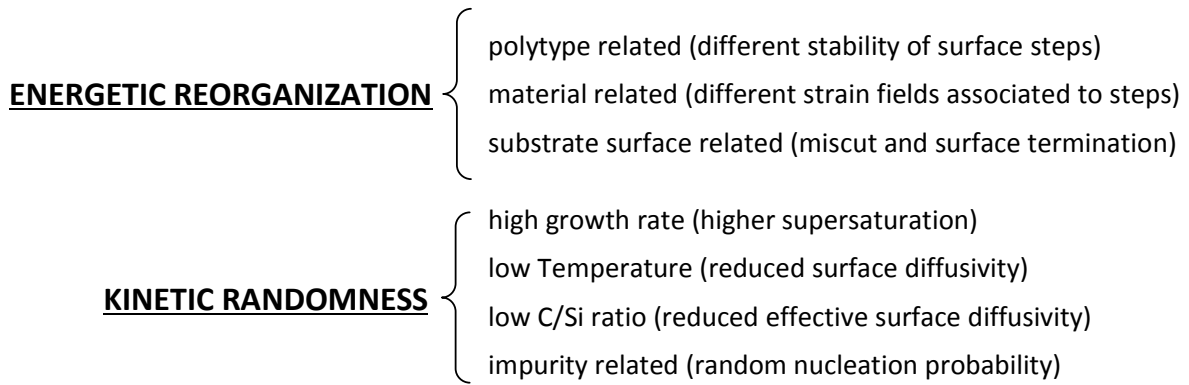


Fig.1 Schematic mechanisms behind energetic vs. kinetic surface organization

Surface analysis

We have analysed the surface morphology of the samples using both SEM, to allow for a complete inspection of the whole film, and AFM, to allow for a qualitative evaluation of the surface roughness (R_q). Fig.2 shows two representative surface morphologies associated to the *lowGr* and *highGr* films. As can be seen, only the first one is affected by a periodic ondulation of the surface, which results in a higher root-mean-square roughness: ~ 1.2 nm to be compared to the ~ 0.3 nm of the *highGr* film.

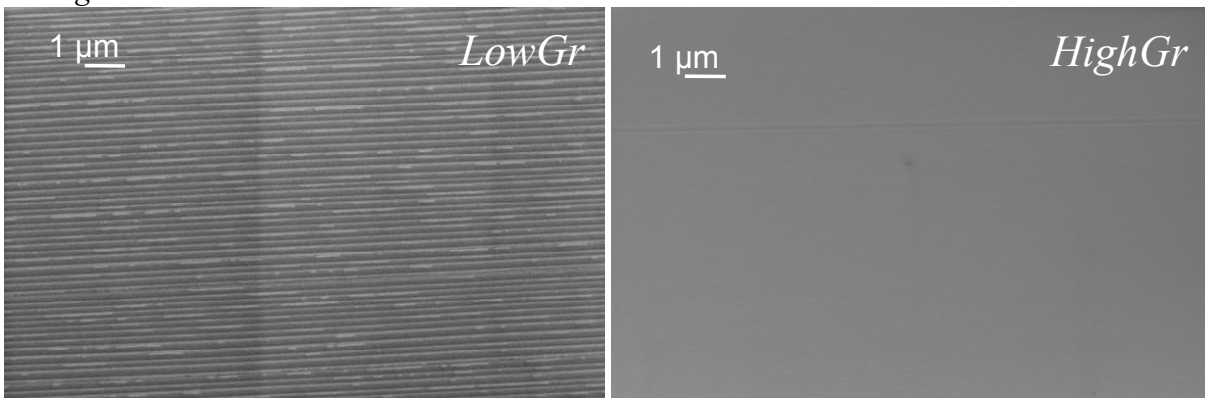


Fig.2 SEM images of the surface for the low (left) and high (right) growth rate samples.

Note that the R_q of an ideal (i.e. without any surface re-organization) 4° degree off 4H-SiC, as can be deduced from simple geometrical considerations, would be equal to:

$$\begin{aligned}
 R_q = RMS &= \sqrt{\left\{ \int_0^{L_T} [z(x)]^2 dx / L_T \right\}} = \sqrt{\left\{ \int_0^{L_T} \left[\frac{h^2}{2L_1^2} x^2 + \frac{h^2}{2L_2^2} (L_T - x)^2 \right] dx / L_T \right\}} = \\
 &= \sqrt{\left\{ \left[\frac{h^2}{L_1^2} \frac{x^3}{3} \right]_0^{L_1} + \frac{h^2}{L_2^2} \left[\frac{(L_T - x)^3}{3} \right]_{L_1}^{L_T} \right\} / 2L_T} = \sqrt{\left\{ \left[\frac{h^2}{3} (L_1 + L_2) \right] / 2L_T \right\}} = h \frac{1}{2\sqrt{3}} = \frac{0.25 \sin(90 - 4)}{2\sqrt{3}} = 0.072 \text{ nm}
 \end{aligned}$$

Thus, even the *highGr* film is affected by surface reorganization, but to a much lower extent compared to the *lowGr* one.

It is interesting to note also that the *highGr* sample shows isolated macro-steps [11] (note the isolated horizontal line in the SEM figure of Fig.2, *right*), these isolated macro-ondulations, which could cause localized electric field crowding and device leakage [12], have been found to disappear by further increasing the growth rate to $60 \mu\text{m/h}$. Work is underway to better characterize this dependency.

These results, together with the observed increase of the surface roughness after high temperature thermal annealing [11] shows that out-of-equilibrium conditions (specifically high growth rates) are indeed capable of hindering the re-organization of the surface during crystal growth.

High temperature Argon thermal treatment

Aiming to better analyze the impact of the energetic reconstruction on the surface morphology and to highlight the crystallographic structure of the fully reconstructed surfaces we have annealed for 30 minutes at $T=1650^{\circ}\text{C}$ and low pressure (20 mbar) in argon ambient two samples grown on substrates with two different miscut directions: the standard one (the $\langle 11-20 \rangle$) and its perpendicular (the $\langle 1-100 \rangle$). This allows to obtain insights on the equilibrium configuration of the steps and surface [22] in both crystallographic directions.

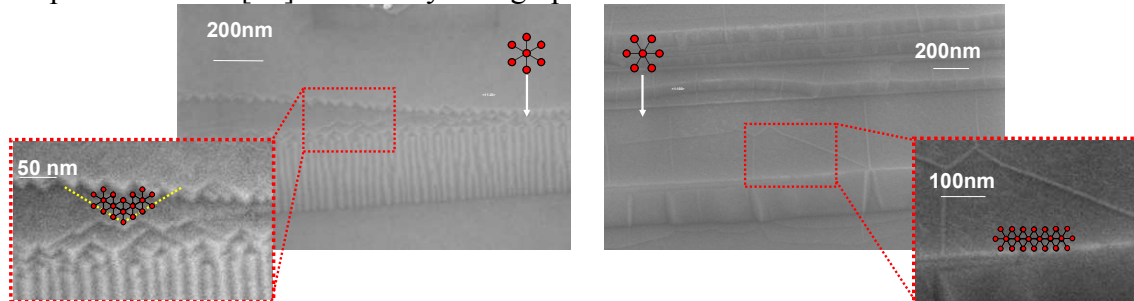


Fig.3 SEM images of the surface steps for the films grown on a $\langle 11-20 \rangle$ (left) and $\langle 1-100 \rangle$ (right) misoriented substrates. This reconstruction as been observed on both as-grown and post-argon annealing. The latter ones show an higher degree of reconstruction, as expected.

As can be seen in Fig.3, the steps present very different morphologies. Step meandering, observed on films grown on $\langle 11-20 \rangle$ misoriented substrates is not present on the film growth on the $\langle 1-100 \rangle$ direction. The two different morphologies are related to the minimization of the surface dangling bonds that tend to align the surface steps towards the $[11-20]$ equivalent direction (see Fig.3 captions). In the case of the $\langle 1-100 \rangle$ miscut direction the steps are already aligned towards the $[11-20]$ direction, so that no reconstruction is needed.

The "tread-to-riser angle"[10,15,16] of the two films as calculated from the height profile measured with AFM has been found to be equal to $\sim 10^{\circ}$ degrees for the $\langle 11-20 \rangle$ direction[9] and to $\sim 20^{\circ}$ degrees for the $\langle 1-100 \rangle$ one, this result reveals the more compact ondulation of the steps for the film grown on $\langle 1-100 \rangle$ misoriented film. Cross sectional TEM analysis are underway to better characterize this result.

Finally, to fully characterize the impact of the growth rate on the film properties we have analyzed the *lowGr* and *highGr* samples using the micro photoluminescence (PL) microscopy[23] to determine the density of single Shockley stacking faults[24] in the two films. Fig.3 shows an intensity map of the room-temperature PL peaks related to the (1,3) stacking faults (which is associated to a peak located 0.2eV below the band gap [25,26 ,27]).

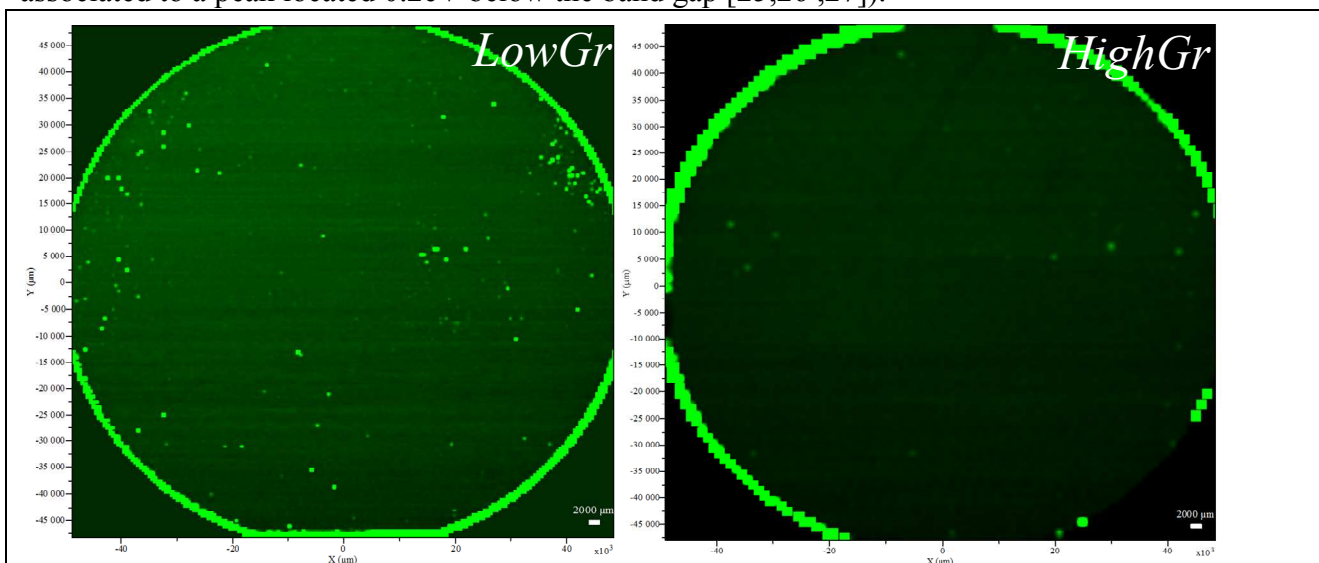


Fig.4 Full 4" inch wafer intensity micro photoluminescence analysis of the (1,3) single Shockley stacking faults (2.91eV) of the *lowGr* and *highGr* samples.

As can be clearly seen in Fig.4, the *highGr* film shows a lower density of single Shockley stacking faults. This is an important and rather unexpected behaviour given that the out-of-equilibrium conditions used in the low R_q sample should favour the generation of defects. On the other hand, a low surface roughness is the result of narrow terraces (see Fig.1 and 2) which are, indeed, capable of hindering the generation of defects and promote homoepitaxy [17,28,29]. The connection between defects generation, surface morphology and growth parameters requires further studies and is currently under investigation.

Monte Carlo simulations

To theoretically explore the connection between surface energy minimization and kinetic randomness we used 3D kinetic atomistic simulations. The algorithm used, named *KsIMC*, is an improvement over standard Monte Carlo algorithms, which usually retain fixed atom positions and bond partners indicative of perfect crystal lattices, this one, instead, relies instead on a refined super-lattice including, within the perfect crystal structure, defective sites identified as complementary sites for each (0001) hexagonal close packed (h.c.p) layer [20]. This allows for a deeper description of the active mechanisms during crystal growth (island nucleation, correlation between the evolution of islands with different symmetry, correlation between the island and step evolution, interaction between bulk and surface structures) and thus a deeper description of the growth kinetics. The probability P_{ij} , for the displacement of a kinetic particle from site "i" to the site "j", is defined using the "bond-counting method":

$$P_{ij} = P_i = \theta_{hop} \exp\left\{-\left(E_{def}n_i^r + E_{reg}n_i^a + R_{LR}E_{LR}\right) / k_B T\right\} \quad (1)$$

where k_B is the Boltzmann constant, T is the system temperature, θ_{hop} is the hopping frequency prefactor, n_i^a and E_{reg} are the number of second (regular) neighbors and the associated bond-strength whereas n_i^r and E_{def} are related to the use of the super-lattice and represent the interaction between the particles in the perfect crystal and those in defective configurations [20]. The $(R_{LR}E_{LR})$ term represents a beyond-second-neighbours interaction on the [0001] direction that distinguishes particle energetic in cubic and hexagonal layers [17,18,19] promoting step bunching[17] and 3C nucleation[21].

To study the surface reorganization as function of the growth rate we have analyzed the terrace width distribution (TWD) of simulated surfaces after homoepitaxial growths. The TWD will be single peaked, with the peak located at the initial terrace width, if no step bunching is present. On the other hand, the step bunching leads to a reorganization of the surface with a splitting of the distribution: one peak located at small terrace widths, associated to the bunched regions, and one located at large terrace widths (larger than the initial one) [2,17]. As can be seen the distribution is single peaked only at high growth rates where kinetic randomness dominate the surface morphology in qualitative agreement with the observed experimental results.

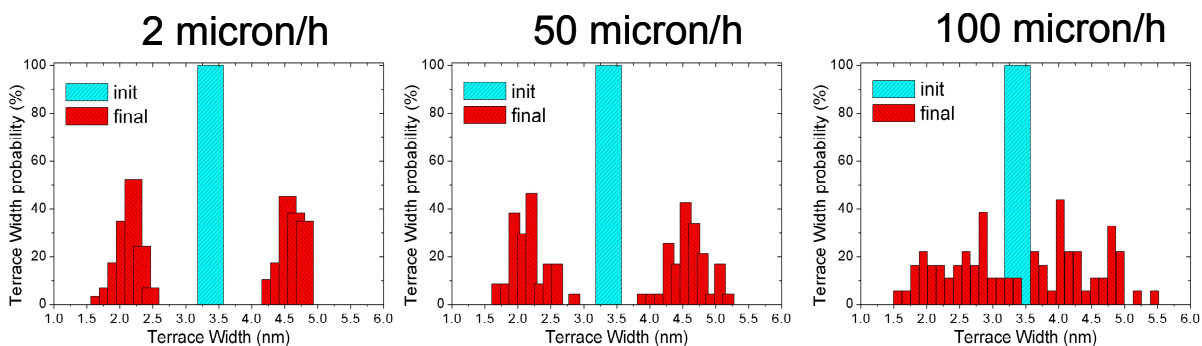


Fig.5 Pre and post-growth terrace width distribution as function of the growth rate (adatom impingement rate). A double peak distribution (present only at low growth rates) is indicative of a reorganized surface.

It is important to note, that atomistic algorithms (such as the one used in this study) are limited in their capability of explore large systems (in this case the computational box was limited to surface areas smaller than 100x100 nm) so that the KsIMC can capture only the first stages of the surface reorganization. This prevents a quantitative theoretical description of the reorganization mechanisms which has a final periodicity of more than ~50 nm).

Summary

By analyzing the surface morphology of "as-grown" and post-annealing 4H-SiC films grown with different growth rate and on different miscut directions of the substrates we explored the interplay between energetic reorganization (which leads to nano-ondulated or step-bunched surfaces) and kinetic randomness, which hinders it. Specifically, for the growth conditions considered (growth temperature $T=1650^{\circ}\text{C}$, C/Si=1.1 grown on $\langle 11\text{-}20 \rangle 4^{\circ}$ off misoriented substrates) an increase of the growth rate from 4 $\mu\text{m/h}$ to 27 $\mu\text{m/h}$ is sufficient to avoid the nano-ondulations and decrease the average surface roughness from ~1.2 to ~0.3 nm. The same deposition conditions showed also a reduction of the single Shockley stacking faults, from ~15 cm^2 to ~5 cm^2 . We compared these results with kinetic Monte Carlo simulations which allow for a theoretical description of the kinetic mechanisms active during homoepitaxial step-flow growths finding the same qualitative trends (surface reorganization for sufficiently low growth rate, i.e. for close to equilibrium conditions).

References

- [1] H. Nakagawa, S. Tanaka and I. Suemune Phys Rev. Lett. **91**, 226107 (2003)
- [2] T. Kimoto, A. Itoh and H. Matsunami, J. Appl. Phys. **66**, 3645 (1995)
- [3] W. Chen and M. A. Capano, Journal of Applied Physics **98**, 114907 (2005)
- [4] J. W. Mullin, Crystallization (Butterworth, London, 1972)
- [5] M. Camarda, A. La Magna, P. Fiorenza, F. Giannazzo and F. La Via, Journal of Crystal Growth **310**, 971 (2008)
- [6] S. Nakamura, T. Kimoto, S. Tanaka, N. Taraguchi, A. Suzuki and H. Matsunami Applied Physics Letters **76**, 3412 (2000)
- [7] M. Camarda, A. La Magna, A. Severino F. La Via Thin Solid Films **518**, S159 (2010)
- [8] H.-C. Jeong and E.-D. Williams Surf. Sci. Rep. **34**, 171 (1999)
- [9] P. Muller and A. Saul Surf. Sci. Rep. **54**, 157 (2004)
- [10] M. Camarda, A. Severino, P. Fiorenza, V. Raineri, S. Scalese, C. Bongiorno, A. La Magna and F. La Via Material Science Forum **679**, 358 (2011)
- [11] M. Camarda, A. Canino, P. Fiorenza, C. Bongiorno, A. Severino, V. Raineri, A. La Magna, M. Mauceri, G. Abbondanza, A. Pecora, and D. Crippa, Material Science Forum **717**, 149 (2012)
- [12] H. Fujiwara, T. Katsuno, T. Ishikawa, H. Naruoka, M. Konishi, T. Endo, Y. Watanabe, K. Tsuruta, S. Onda, A. Adachi, M. Nagao and K. Hamada Material Science Forum **717**, 911 (2012)
- [13] K. K. Lee, T. Ohshima, A. Ohi, H. Itho and G. Pensl Japanese J. App. Phys. **45**, 6830 (2006)
- [14] A.K. Agarwal, S. Seshadri, J.B. Casady, S.S. Mani, M.F. MacMillan, Nelson Saks, A.A. Burk, G. Augustine, V. Balakrishna, P.A. Sanger, C.D. Brandt, R. Rodrigues Diamond and related materials **8**, 295 (1999)
- [15] D. L. Rode, Journal of Crystal Growth **27**, 313 (1974)
- [16] D. L. Rode, W. R. Wagner, and N. E. Schumaker, Applied Physics Letters **30**, 75 (1977)
- [17] M. Camarda, F. La Via, and A. La Magna Surface Science **605**, L67 (2011)
- [18] V. Borovikov and A. Zangwill, Phys. Rev. B **79**, 245413 (2009)
- [19] M. C. Righi, A. Pignedoli, G. Borghi, R. Di Felice, C. M. Bertoni, Phys. Rev. B **66**, 045320 (2002)
- [20] M. Camarda, A. La Magna, and F. La Via, J. Comp. Phys. **227**, 1075 (2007)
- [21] M. Camarda, Surface Science **606**, 1263 (2012)
- [22] M. A. Capano, S. Ryu, M. R. Melloch, J. A. Cooper and M. R. Buss, Journal of Electronic Materials **27**, 370 (1998)

- [23] A. Canino, M. Camarda and F. La Via Materials Science Forum **645**, 555 (2010)
- [24] M. Camarda, P. Delugas, A. Canino, A. Severino, N. Piluso, A. La Magna and F. La Via, Materials Science Forum **645**, 283 (2010)
- [25] W. Choyke, H. Matsunami and G. Pens, *Silicon Carbide: Recent Major Advances* (Springer, Berlin, 2005)
- [26] M. Camarda, A. La Magna, P. Delugas and F. La Via Applied Physics Express **4**, 025802 (2011)
- [27] I. Deretzis, M. Camarda, F. La Via and A. La Magna, Phys. Rev. B **85**, 235310 (2012)
- [28] T. Kimoto and H. Matsunami, J. Appl. Phys. **75**, 850 (1994).
- [29] M. Camarda, La Magna, A. Canino and F. La Via, Surface Science, **604**, 939 (2010)

Silicon Carbide and Related Materials 2012

10.4028/www.scientific.net/MSF.740-742

Study of the Effects of Growth Rate, Miscut Direction and Postgrowth Argon Annealing on the Surface Morphology of Homoepitaxially Grown 4H Silicon Carbide Films

10.4028/www.scientific.net/MSF.740-742.229